

## Title

Elemental analysis for profiling counterfeit watches

## Author names and affiliations

Sarah Hochholdinginger<sup>1</sup>

Michel Arnoux<sup>2</sup>

Pierre Esseiva<sup>1</sup>

Olivier Delémont<sup>1</sup>

<sup>1</sup> School of Criminal Justice, University of Lausanne, 1015 Lausanne, Switzerland

<sup>2</sup> Anticounterfeiting Department, Federation of the Swiss Watch Industry FH, 2502 Biel, Switzerland

## Abstract

Counterfeit watches are products of illicit activity and contain traces of their production and distribution. Traces provide pertinent information through one of their fundamental characteristics: the ability to reveal links between specimens or cases. The aim of this study was to develop an analytical strategy to obtain the elemental composition of watchcases, by analysing a selection of 35 counterfeit watches. We propose a methodology based on multivariate statistical analysis of chemical results that discriminates between watches from common and different origins, and, ultimately, classifies them into chemical groups. All watchcases were analysed using inductively coupled plasma mass spectrometry (ICP-MS), providing representative descriptive data on the composition of watchcases. Several multivariate approaches were assessed, considering different scenarios, each using a different set of variables. It appeared that the model that performed best in terms of classification criteria could be misleading, especially in an exploratory context that focuses on the production of intelligence. At the end of the day, hierarchical cluster analysis (HCA) allowed us to classify the specimens into 14 chemical classes. Information gained through chemical analysis revealed several links between the specimens. This initial study was performed on a very limited number of watches. Although still in the developmental stage, our approach exhibits promising capabilities and encourages chemical profiling of counterfeit watches on larger scale.

## Introduction

Counterfeiting is a major international crime that reaches far beyond luxury goods. It feeds an important illicit market, benefiting from several major driving forces on both the demand and the supply sides: the attractiveness of “fakes” that are considerably less expensive than the genuine products; the ongoing growth of the Internet as a marketing channel; the expansion of world trade; the combination of cheap production costs and high benefits; weak regulatory and enforcement frameworks; and, of course, the demand for counterfeits. The Organisation for Economic Co-Operation and Development (OECD) estimates the international trade in “fakes” was as high as USD 461 billion in 2013, which is equivalent to 2.5% of total international trade [1].

The illicit practice of watch counterfeiting has come under the scrutiny of the Federation of the Swiss Watch Industry (FHS), whose legal and anti-counterfeiting department performs physical examinations of watches suspected being counterfeit [2]. But despite the efforts of the FHS and of other key actors, many questions regarding the traffic of counterfeit watches remain unanswered.

The practice of forensic science relies fundamentally on the study of traces left behind in the course of criminal activity, and on the extraction and contextualization of the information they convey. Beyond its evidentiary contribution in specific court proceedings, forensic science plays other important roles. The information content of traces can contribute to models in which intelligence and crime analysis tend to support strategic decisions and crime prevention [3]. From this perspective, forensic intelligence can significantly advance the understanding of illicit trafficking or hidden markets in general, and the trading of counterfeit goods in particular. When put into context with other types of intelligence gathered through the spatiotemporal analysis of seizures or the monitoring of Internet sites selling such products, the physical and chemical analysis of counterfeit goods may yield valuable knowledge on the structure of this illicit market.

This research investigated whether the elemental composition of watchcases is a useful source of information on the production of counterfeit watches. As the production of watchcases requires expensive machinery, we assumed that only a finite number of production sites, intended to manufacture copies of watch parts, have access to such technology. Watchcases originating from the same production batch are made from the same raw materials and should have the same chemical composition. The proposed methodology consists of the extraction of meaningful chemical information, and its correlation with existing physical information.

Even though chemical profiling methods are not new and have found application in a variety of areas of forensic science, with new methodologies, new questions inevitably

arise. The aims of this study were therefore to: 1) develop an analytical strategy to measure the elemental composition of watchcases; 2) analyse a selection of counterfeit watches; 3) propose a statistical methodology that discriminates between watches of different origins; and 4) classify the watchcases into chemical groups and hence provide new knowledge on the production of the watches. The ultimate objective was to lay the groundwork for the further use of the data in a forensic intelligence perspective.

## Material and methods

### Specimen set and analytical strategy

The specimen set consisted of 35 counterfeit watches (labelled *M01* to *M35*), including seven models of a commonly counterfeit brand<sup>1</sup>, obtained from the Federation of the Swiss Watch Industry (FHS). The watches had been seized by customs authorities at the Swiss border, and had been previously identified as counterfeits, and analysed, by the FHS. Physical analysis included measurements of corporate logos and trademarks on the different watch parts. Seizure information, including place and date of seizure, as well as origin and ways of transit, if known, was also recorded. The group of specimens was especially selected to comprise watches of only one brand, seized during a relatively short period of time (7 months), in order to increase the chances of finding chemical and physical links between the specimens. Intuitively, it is more likely that the same raw materials and the same tools were used. Limiting the specimen set to a single brand thus increased the chances of gathering information on illicit networks.

All watches were disassembled by FHS specialists, and only the watchcases were chosen as objects of study. The watchcases were almost exclusively made of metal, which dictated the analytical method.

First, X-ray fluorescence (XRF) was used as a screening technique to identify the type of alloy. Inductively coupled plasma mass spectrometry (ICP-MS) was then utilized to obtain the elemental composition of the watchcases. ICP-MS has been used to analyse jewellery [4, 5] as well as to determine the trace-metal composition of steel [6]. Table 1 summarizes the major and minor elements that were quantified. Several isotopes per element were considered, to detect possible isobaric or polyatomic interferences.

---

<sup>1</sup> Due to brand confidentiality requirements, no image or detailed information on the counterfeit watch specimens is disclosed

Table 1: List of the major and minor elements and corresponding isotopes analysed by ICP-MS.

	<b>Element</b>	<b>Isotopes</b>
<b>Major elements</b>	Chrome (Cr)	52
	Iron (Fe)	54, 56
	Nickel (Ni)	58, 60
	Aluminium (Al)	27
	Silicon (Si)	28
	Phosphorus (P)	31
	Titanium (Ti)	48, 49
	Vanadium (V)	51
	Manganese (Mg)	55
<b>Minor elements</b>	Cobalt (Co)	59
	Copper (Cu)	63, 65
	Zinc (Zn)	66
	Arsenic (As)	75
	Molybdenum (Mo)	95, 98
	Cadmium (Cd)	112, 114
	Tin (Sn)	118
	Tungsten (W)	182, 183
	Lead (Pb)	206, 207, 208
	Uranium (U)	238

## Reagents

Nitric acid ( $\text{HNO}_3$ , >69.0%, TraceSelect, Fluka Analytical) and hydrochloric acid ( $\text{HCl}$ , >37%, TraceSelect, Fluka Analytical) were used. High-purity argon gas was used for the ICP-MS system (purity > 99.999%, ALPHAGAZ). Certified single-element standards ( $1000 \mu\text{g mL}^{-1}$ ) for aluminium (Al), chromium (Cr), manganese (Mn), iron (Fe), cobalt (Co), nickel (Ni), copper (Cu), zinc (Zn), arsenic (As), cadmium (Cd), tin (Sn) and lead (Pb) were purchased from CentriPUR, Merck. Certified single-element standards ( $1000 \mu\text{g mL}^{-1}$ ) of phosphorus (P), silicon (Si), titanium (Ti), vanadium (V), molybdenum (Mo) and tungsten (W) were purchased from TraceCert, (Sigma-Aldrich). Finally, a certified single-element standard ( $1000 \mu\text{g mL}^{-1}$ ) of uranium (U) was purchased from Inorganic Ventures, Inc. For internal standards, scandium (Sc), germanium (Ge), yttrium (Y), rhodium (Rh), indium (In), terbium (Tb) and bismuth (Bi) ( $1000 \mu\text{g mL}^{-1}$ ) were used (CentriPUR, Merck). Ultrapure water ( $18.2 \text{ M}\Omega/\text{cm}$ ) was prepared with an ELGA PURELAB Ultra instrument.

## Sample preparation, analytical method and validation

Five samples (approximately 1 g each) per watchcase were cut by electrical discharge. They were pre-digested during a cleaning step to remove surface plating and contaminants generated during the cutting process. The cleaning was performed in open Falcon tubes (15 ml) containing a 3:1 mixture of  $\text{HCl}$  and  $\text{HNO}_3$ , for 30 to 40 min. The samples were then transferred into quartz tubes containing 6 ml  $\text{HCl}$ , 1 ml  $\text{HNO}_3$  and 6 ml high-purity deionized Milli-Q water ( $>18.2 \text{ M}\Omega/\text{cm}$ , ELGA water

systems). Microwave-assisted acid digestion was performed in a PTFE vessel on a turboWAVE 1500 system (Mikrowellensysteme MWS). The digestion steps for the microwave are summarized in Table 2.

The quantitative analysis of major elements required a 1:250,000 dilution in 1% HNO<sub>3</sub>, and the analysis of minor elements required a 1:1,000 dilution; these were performed with a microLAB 600 series (Hamilton) diluter. Internal standards were then added to the samples. The quantitation of major and minor elements required the performance of two separate analyses, due to large differences in the concentration ranges of the major and trace elements. To eliminate or reduce the effect of interferences, both collision-reaction interface (CRI) gases (He and H<sub>2</sub>) were used. Elemental concentrations were then measured with a Bruker Aurora M90 ICP-MS, applying the operating conditions detailed in Table 3.

Table 2: Microwave oven program for the complete digestion of the steel samples

Step	t [min]	MW [W]	T [°C]	P [bar]
1	5	1000	180	120
2	5	1200	220	150
3	20	1200	220	150

Table 3: Operating conditions for ICP-MS

ICP-MS		Aurora M90 (Bruker)
Spray chamber		Peltier-cooled (3°C), double-pass Scott type
Nebulizer		Quartz MicroMist Low Flow Unifit (0.4 ml·min <sup>-1</sup> )
Cones		Nickel
RF Power [kW]		1.45
Gas Flow [L·min <sup>-1</sup> ]	Plasma flow	18.00
	Auxiliary flow	1.80
	Nebulizer flow	1.00
Sample introduction	Sampling depth [mm]	5
	Pump rate [rpm]	5
	Stabilization time [s]	30
Quadrupole scan	Scan mode	Segmented scan
	Dwell time [ms]	10
Attenuation mode		None
Acquisition	Points per peak	1
	Scans/ Replicate	30
	Replicates/ Sample	5
Washing solution		HNO <sub>3</sub> 1%
Washing time [s]		10
Collision reaction interface		H <sub>2</sub> : 90 mL/min He: 110 mL/min

The analytical method was then validated. Along this process, several elements, isotopes or CRI gas conditions were removed to keep only the most reliable variables for the chemical profiles.

### **Data analysis**

Four scenarios, each including a different set of variables, were selected. The aim of this process was to assess the impact of variable selection on the ensuing multivariate data analysis. Strategies to assess intra- and inter-source variations, in absence of specimens where a common source is assured, were studied and applied. The different scenarios were then evaluated in terms of classification performance, and a threshold value to discriminate specimens was determined.

The final step consisted of the visualisation of the grouping of the counterfeit watches. This was achieved through cluster analysis (CA), one of the recommended methods to obtain better insight into the structure of data [7]. This method summarises a data set in a two-dimensional graphical form and allows specimens to be grouped into clusters based on measures of distance and similarity. Thus, specimens with similar characteristics in the variable space are grouped in the same class. The distance between two points in the  $n$ -dimensional space was computed using the Euclidian distance. Among the several clustering methods that exist [8], we opted for the common method of hierarchical cluster analysis. Specimens were portioned into  $k$  clusters ( $k = 1, \dots, n$ ) whose grouping is visualized in a hierarchical dendrogram. The horizontal axis represents the distance between two points. Specimens from a cluster of a lower level in the hierarchy are a subset of those from higher levels [7]. Therefore, the threshold distance, at which the grouping is stopped, determines the number of clusters in the final classification.

Data processing was performed using Microsoft Excel 2016, R (version 3.4.2) in combination with RStudio (version 1.1.383).

## **Results and discussion**

### **Analytical results and method validation**

All watches, except for one specimen (*M01*), were made of austenitic stainless steel, meaning that Fe, Cr and Ni were the major components [9]. XRF analysis revealed that *M01* was made of a Zn-Cu-Ni alloy and this specimen was not considered for further ICP-MS analysis, since the dissolution matrix was developed for steel. Visual examination of the watches indicated that they were of relatively high quality, with mechanical movements found in higher-quality counterfeits. It should be noted that watches of poorer quality may be made of alloys other than steel.

Analytical difficulties occurred for P and Si, and no results could be gathered. Cd and U were not found ( $< \text{LOD}$ ) in any of the specimens, and were therefore not considered. Pb207(He) was excluded because of the high percentage of relative standard deviation (%RSD) of the slope when considering linearity.

As the precision of the determination of the concentration of single elements is a key factor when dealing with chemical profiles, repeatability was tested both on a control sample (midrange certified calibration solution), and on a counterfeit watch specimen (*M20*). It was found that Al(He), Ti(H<sub>2</sub>), Co(He), Cu(H<sub>2</sub>), Mo(He and H<sub>2</sub>) showed high values of %RSD ( $>8$ ), based on multiple analyses of control samples; these were therefore excluded. Zn showed extremely high %RSD in the watch specimens, and was also discarded. The remaining elements showed satisfactory results, as shown in Table 4. Pb was not detected in watch specimen *M20*.

Due to the lack of suitable certified reference material, we used certified calibration solutions to test accuracy. The recovery values indicated that the elements determined by ICP-MS agreed with the certified values (Table 5). Internal standardization was used to correct matrix effects. Also, all samples were considerably diluted, decreasing the acidification of the sample and, therefore, matrix effects associated with viscosity changes.

Table 4 : Repeatability of the analysed elements

Element	Control sample		Watch specimen M20	
	Repeatability [%]	# Meas.	Repeatability [%]	# Meas.
Al(H2)	9.67	24	14.89	4
Ti(He)	5.47	48	11.50	8
V(He)	5.43	24	2.12	4
V(H2)	2.93	24	2.06	4
Mn(He)	4.55	24	2.01	4
Mn(H2)	3.93	24	3.51	4
Co(H2)	2.76	24	2.43	4
Cu(He)	4.67	24	3.75	4
As(He)	4.28	24	8.84	4
As(H2)	4.67	24	9.42	4
Sn(He)	2.78	24	1.04	4
Sn(H2)	2.96	24	2.83	4
W(He)	4.11	48	5.06	8
W(H2)	4.91	48	2.28	8
Pb(He)	3.39	48	N/A	-
Pb(H2)	2.57	72	N/A	-

Table 5: Accuracy assessment of the method

Element	Certified conc. [ppb]	Mean measured conc. [ppb]	Recovery [%]
Al(H2)	10	9.00 ± 0.97	90.00
Ti(He)	10	10.23 ± 0.55	102.28
V(He)	200	214.90 ± 10.86	107.45
V(H2)	200	187.40 ± 5.86	93.70
Mn(He)	4000	4225.85 ± 182.10	105.65
Mn(H2)	4000	4029.53 ± 157.21	100.74
Co(H2)	1000	984.47 ± 27.65	98.45
Cu(He)	200	197.04 ± 9.34	98.52
As(He)	10	10.05 ± 0.43	100.46
As(H2)	10	10.30 ± 0.47	103.02
Sn(He)	5	5.07 ± 0.14	101.45
Sn(H2)	5	4.98 ± 0.15	99.58
W(He)	20	19.47 ± 0.82	97.35
W(H2)	20	18.00 ± 0.98	90.00
Pb(He)	5	4.89 ± 0.17	97.86
Pb(H2)	5	4.91 ± 0.13	98.26

In total, ten elements, encompassing 23 combinations of isotopes and gas conditions, were validated, and retained as potential variables for the construction of the chemical profile.

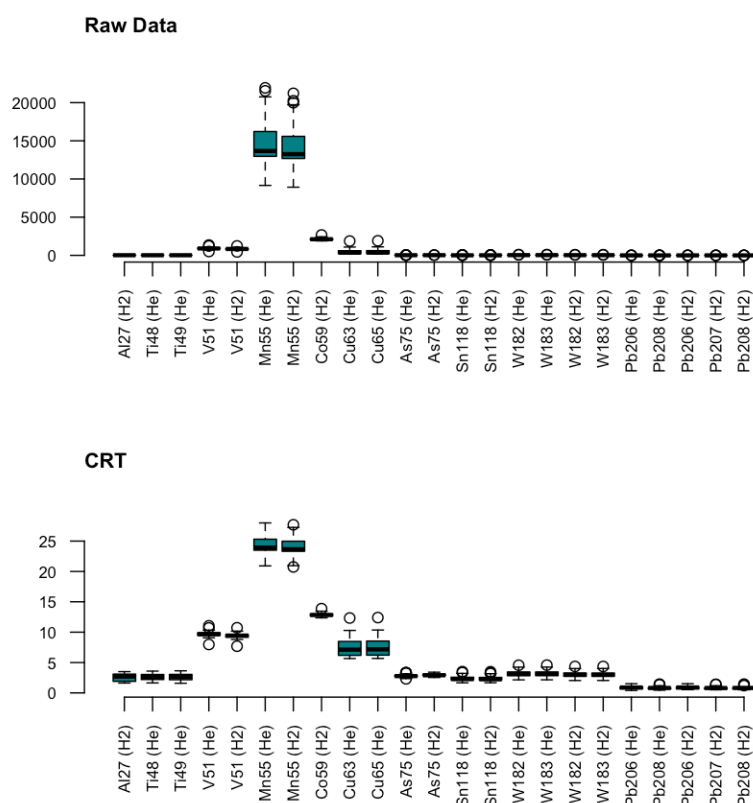
### Variable selection and multivariate data analysis

It is conceivable that the composition of the major constituents of steel alloys is very similar in watchcases from different production lines. Thus, better linking and/or separation of specimens might be achieved through the exploitation of trace-element profiles. Hence, we decided to rely on the minor elements for the profiling of the



watchcases. Exploration of raw ICP-MS data revealed large differences in the concentrations of the minor elements. In order to obtain better symmetry, data pre-processing was needed [7]. We took care to maintain analytical information and to prevent amplifying the background noise, which would disproportionately influence errors of measurement. After testing several pre-processing techniques, we decided to scale the data using a cube root transformation (CRT) (Figure 1) to decrease the influence of elements present in high concentrations.

Figure 1 : Boxplots showing the variability of all variables in the raw data and on pre-processed data after cube root transformation (CRT)



All elements were analysed with two different CRI gases (He and H<sub>2</sub>), to minimize possible isobaric and polyatomic interferences. A single variable per element, gas condition and isotope had to be chosen to avoid overweighting certain elements. The selection criteria were the following:

- Lowest overall %RSD for all replicates of the 34 analysed watchcases, since homogeneity is essential in a profiling context.
- If %RSDs were comparable, the most abundant isotope.

A total of 10 elements, listed in Table 6, were retained for further multivariate data analysis.

Table 6 : Selection of variables according the mean overall %RSD of all replicates and natural abundance of isotopes

Element	Gas condition	Isotope	Mean overall RSD [%]	Natural abundance [%]	Selection	
Al	H <sub>2</sub>	27	12.53	100	<sup>27</sup> Al (H <sub>2</sub> )	
Ti	He	48	7.57	73.72	<sup>48</sup> Ti (He)	
	He	49	10.19	5.41		
V	He	51	1.64	99.75	<sup>51</sup> V (He)	
	H <sub>2</sub>	51	1.93			
Mn	He	55	1.55	100	<sup>55</sup> Mn (H <sub>2</sub> )	
	H <sub>2</sub>	55	1.37			
Co	H <sub>2</sub>	59	1.74	100	<sup>59</sup> Co (H <sub>2</sub> )	
Cu	He	63	3.37	69.17	<sup>63</sup> Cu (He)	
	He	65	3.35	30.83		
As	He	75	5.97	100	<sup>75</sup> As (He)	
	H <sub>2</sub>	75	7.64			
Sn	He	118	2.76	24.22	<sup>118</sup> Sn (H <sub>2</sub> )	
	H <sub>2</sub>	118	2.02			
W	He	182	7.85	26.5	<sup>182</sup> W (H <sub>2</sub> )	
	H <sub>2</sub>	182	7.52			
	He	183	7.76			14.31
	H <sub>2</sub>	183	7.44			
Pb	He	206	15.59	24.1	<sup>208</sup> Pb (H <sub>2</sub> )	
	H <sub>2</sub>	206	3.87			
	H <sub>2</sub>	207	4.56			22.1
	He	208	13.75			52.4
	H <sub>2</sub>	208	3.72			

Four different scenarios, comprising combinations of the selected variables, were then evaluated. Scenario 1 took all ten variables into consideration (Al, Ti, V, Mn, Co, Cu, As, Sn, W, Pb). The variables for scenario 2 were V, Mn, Co, and Cu, as these were measured at the highest concentration (> 100 ppb) and are the most likely to be remeasured again in future steel case samples. For scenario 3, we retained Al, Ti, As, Sn, and W, as their concentrations were in a comparable analytical range (10-100 ppb), which reduces the influence of very high or very low concentrations. Scenario 4 comprised V, Mn, Co, Cu, As, Sn, elements with the lowest overall %RSD, because these were potentially the most homogeneously distributed elements within the watchcases.

### Inter- and intravariability assessment and evaluation of the different scenarios

Since we sought to link watchcases from a common source and discriminate these from watchcases from different sources, inter- and intra-source variations needed to be studied. Given the fact that we did not have access to seizures with a formal indication of a common source, intra-source variation had to be determined by other means. One way was to look at the variation within the samples cut from a same specimen. To assess inter-replicate similarity, five replicate samples per watchcase were analysed.

The underlying assumption was that variability within a specimen reflects variability between specimens of a common source.

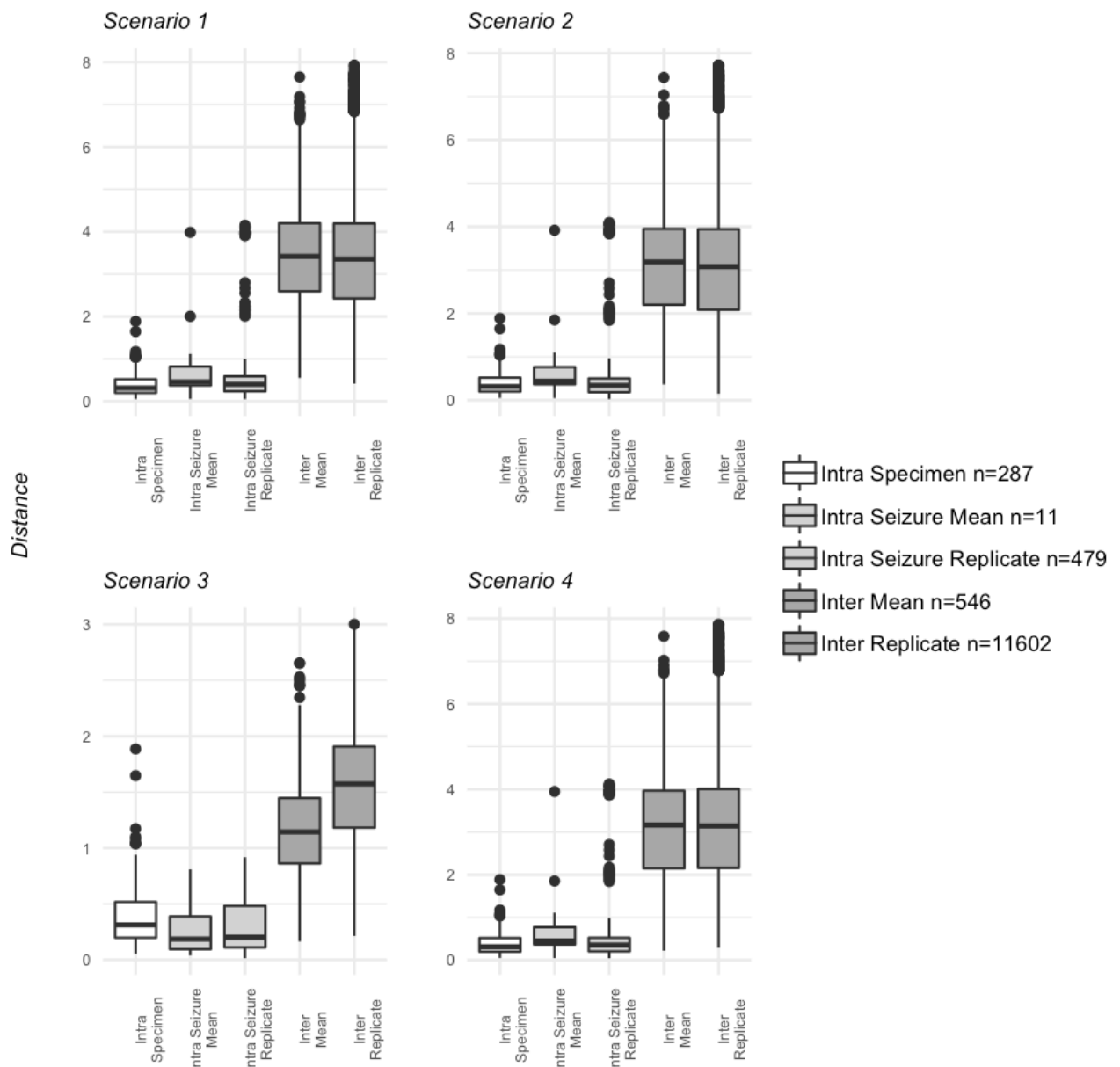
Another way to determine common source was to consider watches that were seized together. Some of these watches were very similar, based on visual examination, technical features (e.g. movement and functionalities) and physical profiling. We assumed that these particular seizures arose from a common production source. Five groups comprising 14 watches, indicated in Table 7, fulfilled these requirements.

Table 7: Groups of counterfeit watches belonging to the same seizure and being non-distinguishable on the basis of technical features and visual examination

<b>Seizure group</b>	<b>Specimen code</b>
1	<i>M09 M10 M11 M12</i>
2	<i>M13 M25</i>
3	<i>M14 M15</i>
4	<i>M26 M27</i>
5	<i>M28 M29</i>
6	<i>M30 M31</i>

Intra- and intervariability distributions were computed by measuring the Euclidean distance between sample pairs from a specific specimen (*specimen intravariability*), between sample pairs from different watches but the same seizure group (*seizure intravariability*) and between sample pairs from unrelated seizures (*intervariability*). It is, however, important to stress that an unrelated seizure context does not mean that two specimens could not be linked. For both *seizure intravariability* and *intervariability* distributions, we considered the mean value of the five samples per specimen, as well as all the five samples, for the four aforementioned combinations of variables (scenarios). The obtained distributions are presented in Figure 2.

Figure 2 : Representation of the distribution of intra- and intervariability according to the selected scenario



In all four scenarios we can observe that *specimen intravariability* is low, whereas the *intervariability* between specimens from unrelated seizures is high. This indicates a separation between intra- and intervariability, and therefore the possibility of distinguishing watchcases from common and different production sources based on measurements of their elemental composition.

Scenarios 1, 2 and 4 appeared to be resistant to change, considering mean values or all samples, although the number of comparisons is much larger. Scenario 3 was more sensitive to change, possibly because the elements were less homogeneously distributed and/or were present in very small concentrations. In consequence, the risk of measurement errors was higher.

Classification required the definition of a threshold value to decide whether watchcases should be grouped or not, based on their chemical profile. Threshold values strongly depend upon the context [10]. If evidence is to be presented to a court, for example, the strategy is to minimize the false positive (FP) rate and therefore the risk of producing erroneously incriminating evidence. In an intelligence-based perspective, the goal is to maximize the true positive (TP) rate. If a link does exist, we do not want to exclude it from further evaluation. Consequently, a number of false positives are also included. The *specimen intravariability* approximates the unknown true production intravariability. We assume production intravariability to be larger or at least equal to *specimen intravariability*. On these grounds, our strategy was to set the threshold values for each scenario at the maximum distance computed for *specimen intravariability*.

The sensitivity (true positive rate) and specificity (true negative rate) of each scenario was evaluated, using previously determined threshold values (Figure 3).

Another performance criterion of a binary classification model is the receiver operating characteristic (ROC) curve. Determination of the ROC curve requires plotting the true positive rate against the false positive rate as the threshold changes; the area under the curve (AUC) is considered a measurement of the accuracy of predictive distribution models. Table 8 summarizes all these metrics for the four scenarios.

Figure 3 : Sensitivity (true positive rate) in black and specificity (true negative rate) in red versus the cut-off distance. The dashed blue line represents the highest *specimen intravariability* value that was found for each scenario and was set as a threshold.

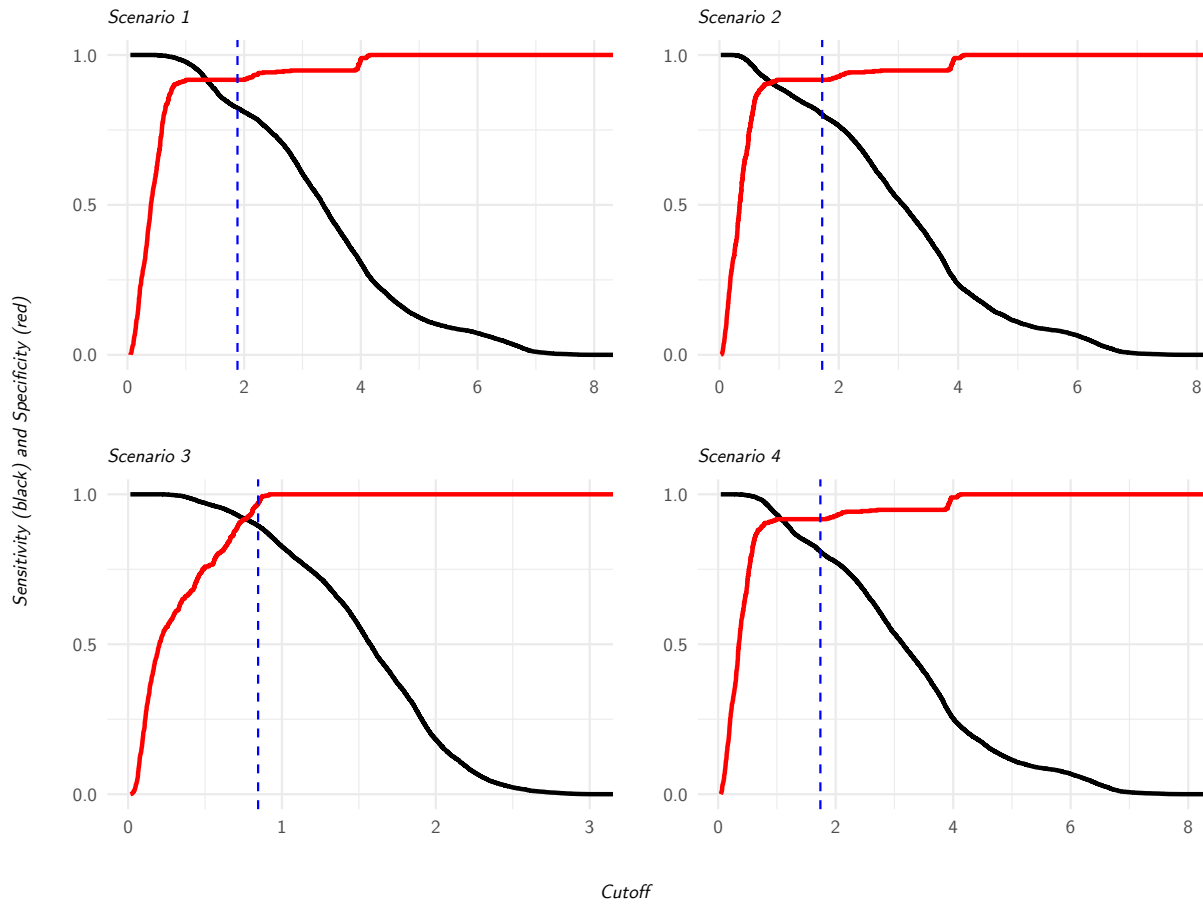
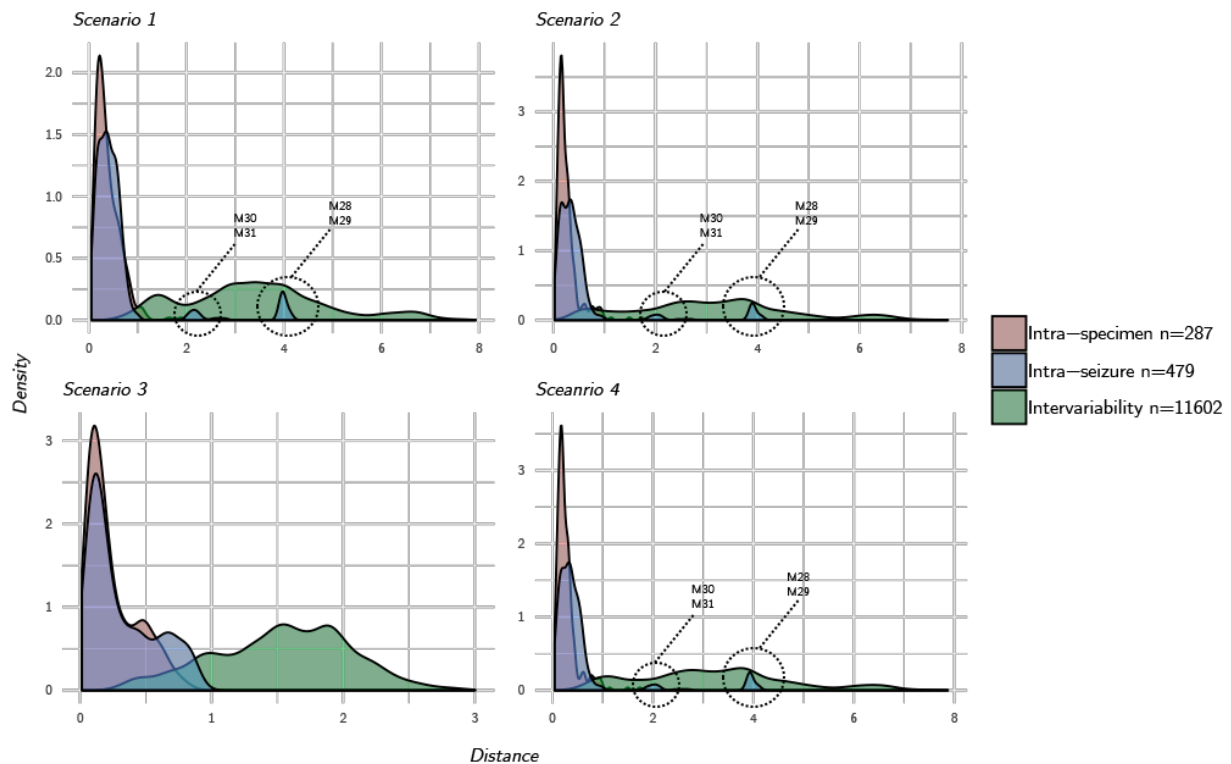


Table 8 : Evaluation criteria for the considered scenarios including the threshold, sensitivity and specificity at the given threshold and the AUC of the ROC curve

	<b>Threshold</b>	<b>Sensitivity</b>	<b>Specificity</b>	<b>AUC</b>
Scenario 1:	1.886	0.917	0.823	0.956
Scenario 2:	1.723	0.917	0.801	0.942
Scenario 3:	0.845	0.969	0.895	0.981
Scenario 4:	1.74	0.917	0.809	0.952

The best performing model was Scenario 3, which considered the five variables whose concentrations were in a comparable analytical range (10-100 ppb). For the given threshold values, sensitivity, specificity and AUC were higher in that scenario than in the others. The AUC for all four models was above 0.94, meaning that each scenario has the potential to reliably classify new specimens of watchcases. Scenarios 1, 2 and 4 did not exhibit significant differences and seemed to provide the same outcomes. Hence, further consideration was given to the distribution of *seizure intravariability*, and its comparison with the *specimen intravariability*, as well as *intervariability*, as shown in Figure 4.

Figure 4 : Distribution plots for all scenarios showing *specimen intravariability*, *seizure intravariability* and *intervariability*

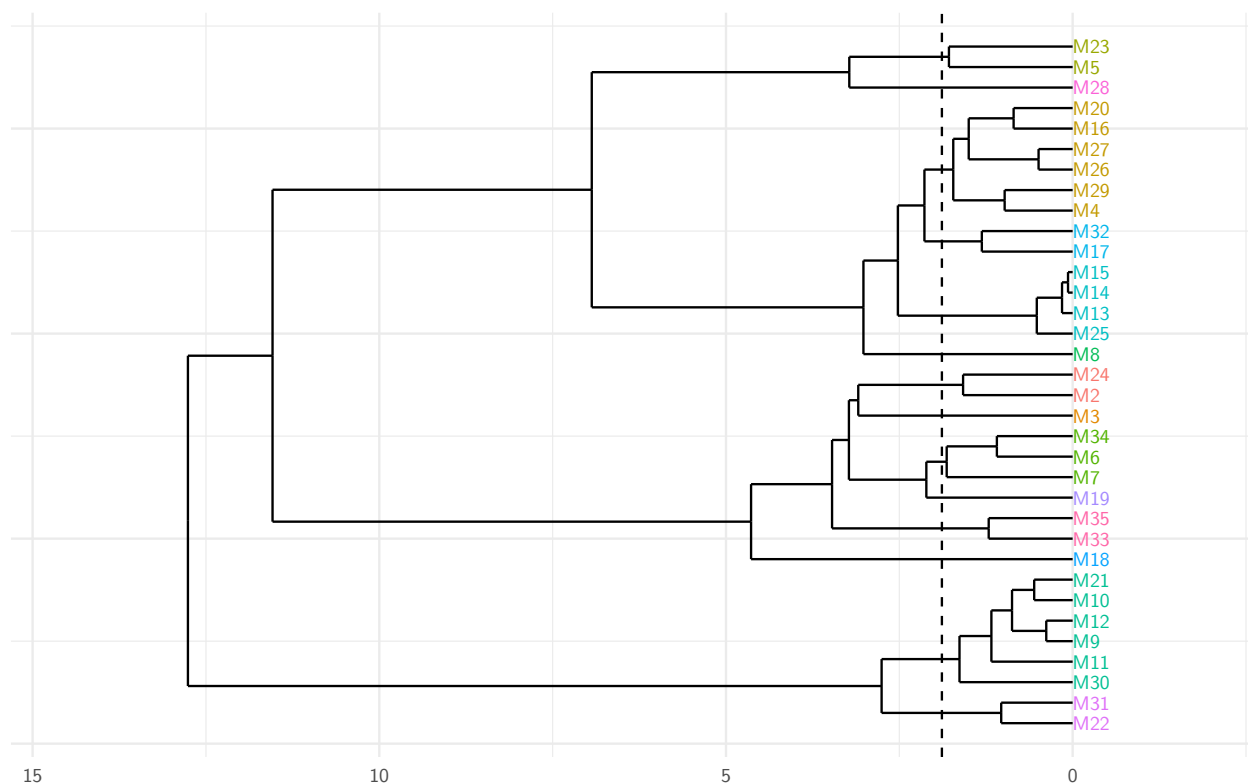


We observed good correspondence between the two different types of intravariability that were computed. This means that most of the watches that were similar, based on physical and seizure-related information, also showed high similarity in their chemical profile. The common thread of Scenarios 1, 2 and 4 is the inclusion of Mn, Co and Cu, the most abundant of the minor elements, in the profile. The distribution curves exhibit similar shapes, indicating that these three elements contribute the most to the distance measurements. Nevertheless, we observed two small peaks at distances of approximately 2 and 4. We found that these peaks corresponded to the watch pairs *M28/M29* and *M30/31*. These two pairs clearly laid within the intervariability distribution, suggesting they should not be linked. In Scenario 3, the two watch pairs are not excludable and would therefore be linked. It is almost possible to superimpose *specimen* and *seizure intravariability*. The only *seizure intravariability* values that were a little higher than the *specimen intravariability* were some values found in another seizure group, namely the group containing watches *M09/M10/M11/M12*. This group is completely absorbed within the *specimen intravariability* in the three other scenarios. It would not be reasonable to choose Scenario 3 for chemical profiling, even though classification performance is better.

The elements Mn, Cu and Co were abundant, and showed very low overall %RSD, indicating a homogeneous distribution within the alloy. They were therefore important profiling variables. The difference in variable selection between the three remaining

scenarios had very little influence on performance criteria. However, Scenario 1 appeared to have slightly better specificity and AUC. We therefore decided to choose Scenario 1 for further evaluations, including all ten variables and using a distance of 1.886 as the threshold value for clustering. The underlying premise for the classification process was that all watchcases separated by a distance lower than the threshold value were produced from the same source. The dendrogram obtained from the hierarchical cluster analysis (HCA) is shown in Figure 5. The defined threshold value allowed the construction of 14 groups, now defined as chemical classes.

Figure 5 : Dendrogram showing the results of the HCA for all specimens (mean value of the five replicate samples per specimen), considering all 10 elements for the chemical profile. 14 chemical groups (indicated in colours) emerged when cutting the dendrogram at the threshold value based on *specimen intravariability*.



We observed a large number of chemical classes ( $N = 14$ ) compared to the number of specimens ( $N = 34$ ). One possible explanation is that the production of the watchcases took place at multiple production sites. It is assumed that the alloys are bought in large quantities and that a physical profile should last over a certain period. Moreover, the specimen set included watches that were seized during a relatively short period, which increases the chances of finding chemical links between them. It should also be noted that the production time of a watchcase may not necessarily be correlated to the time a watch or a group of watches is seized by authorities. However, we were able to show that in some cases watches belonging to the same seizure and with established physical links were chemically as similar as replicate samples from a same specimen. The high number of chemical classes is not surprising, taking into consideration the



fact that the examined brand is one of the most counterfeited in the luxury watch segment.

## **Discussion**

The number of analysed specimens was very limited, simply because of the complexity of the preparation for analysis. Future studies would benefit from considering more specimens. An additional downside was the use of watches seized by custom authorities. These watches had already gone through the complete process of production, assembly, distribution towards a marketplace and final purchase. In the course of this process, information on a common source was associated with more and more uncertainties. It would therefore be very useful to have access to counterfeit watches which are already known to originate from the same source, e.g. from seizures conducted at different production sites. With such specimens, intravariability could be evaluated by computing the distribution between pairs from the same production site and intervariability by computing the distribution from the ones of different production sites. The distributions of intra- and intervariability would possibly be influenced by a new specimen, and threshold values would have to be reevaluated [11].

Developing appropriate countermeasures against the traffic of counterfeit watches requires the understanding of this phenomenon from various points of view. It is of crucial importance to comprehend the level of intelligence that traces and information may provide. In our case, the trace was the elemental composition, providing information on the production of alloys used for counterfeit watchcases. Although the sample preparation was laborious, the analytical results were very satisfactory. Hence, the analytical strategy may be generalized to other applications where the bulk composition of steel products is of interest. Nonetheless, the analytical strategy should be subject to further assessment with larger sets of specimens.

Chemical profiling in terms of multivariate data analysis and structuring of analytical results revealed several links between counterfeit watches. The utility of these links in terms of added intelligence value was assessed through the integration of these chemical profiling results with other types of information pertaining to physical features of the counterfeit watches and with spatiotemporal data of their seizures. The output of this process was that some of the chemical links corroborated existing knowledge, while others revealed new connections between different seizures and specimens. This suggests that additional information can be gained through the chemical profiling of watchcases. This will be further developed in a forthcoming article. Another interesting aspect related to the contribution of chemical profiling of counterfeit watches is that the methodology could be extended to detect brand-independent links, which is rarely possible with physical profiling.

## Bibliography

1. *Trade in Counterfeit and Pirated Goods: Mapping the Economic Impact*. 2016, OECD/EUIPO: Paris.
2. *Annual Report*. 2015, Federation of the Swiss Watch Industry
3. Ribaux, O., et al., *Forensic Intelligence*, in *Professional Issues in Forensic Science*, M. Houck, Editor. 2015.
4. Streicher-Porte, M., A. Buckenmayer, and S. Pfenninger, *What goes around comes around? High levels of cadmium in low cost jewelry*. 2008 IEEE International Symposium on Electronics and the Environment, 2008: p. 1-5.
5. Cox, C. and M. Green, *Reduction in the prevalence of lead-containing jewelry in california following litigation and legislation*. *Environmental Science and Technology*, 2010. **44**(16): p. 6042-6045.
6. Finkeldei, S. and G. Staats, *ICP-MS – A powerful analytical technique for the analysis of traces of Sb, Bi, Pb, Sn and P in steel*. *Fresenius' Journal of Analytical Chemistry*, 1997. **359**(4): p. 357-360.
7. Varmuza, K. and P. Filzmoser, *Introduction to multivariate statistical analysis in chemometrics*. 2009: CRC press.
8. Miller, J.N. and J.C. Miller, *Statistics and chemometrics for analytical chemistry*. 2010: Pearson Education.
9. Hosford, W.F., *Iron and steel*. 2012: Cambridge University Press.
10. Esseiva, P., et al., *Illicit drug profiling, reflection on statistical comparisons*. *Forensic Science International*, 2011. **207**(1-3): p. 27-34.
11. Cadola, L., J. Broséus, and P. Esseiva, *Chemical profiling of different hashish seizures by gas chromatography-mass spectrometry and statistical methodology: A case report*. *Forensic Science International*, 2013. **232**(1-3): p. e24-e27.